The Annals of the University Dunarea de Jos of Galati
Fascicle VI – Food Technology (2024), 48(2), 45-61

ORIGINAL RESEARCH PAPER

WATER ACTIVITY AS A DETERMINANT OF CHANGES IN PHYSICAL AND CHEMICAL PROPERTIES OF *WALANG* LEAVES (*ETLINGERA CF. WALANG* (BLUME) R.M.SM) DURING DRYING USING VARIOUS METHODS

SITI MUJDALIPAH[1,2], DIDAH NURFARIDAH[1,3], DASE HUNAEFI[1,3], TJAHJA MUHANDRI[1,3], NURI ANDARWULAN[1,3*]

[1]*Department of Food Science and Technology, IPB University, Bogor 16680, Indonesia.*
[2]*Food Technology Study Program, Faculty of Technical and Industrial Education, Universitas Pendidikan Indonesia, Bandung 40154, West Java, Indonesia.*
[3]*South-East Asia Food and Agricultural Science and Technology (SEAFAST) Center, IPB University, Bogor, Indonesia.*
*Corresponding author: andarwulan@apps.ipb.ac.id

Received on 29 August 2024
Revised on 31 October 2024

Abstract

Water activity (a_w) plays a crucial role in controlling microbial growth and chemical reactions in food products. This study explores the impact of a_w on the physical and chemical properties of *walang* leaves dried using five different methods: sun drying (SD), sun drying with fan (SDF), fluidized bed drying (FBD), air drying (AD), and freeze drying (FD). The drying methods produced varying drying rate equations. The Wang and Singh model was identified as the most suitable for describing the drying rate. Moisture sorption isotherm (MSI) models varied, with SDF and AD aligning with the Hasley model, SD (Oswin model), and FBD (GAB model). Significant changes in moisture content, color, total phenolic content (TP), and antioxidant activity (AA) were observed across different a_w zones, particularly in zone III. The Dunnett test revealed significant differences in TP, L*, and ΔE between dried leaves and FD controls ($p<0.05$), but no significant differences in MC, a_w, color attributes, or AA ($p>0.05$). SD was recommended for drying *walang* leaves due to its comparable AA and the fastest drying rate.

Keywords: antioxidant activity, sun drying, walang leaves, water activity

Introduction

Walang plant (*Etlingera cf. walang* (Blume) R.M.Sm) can be massively found in Regency of Serang, Banten, Indonesia. Poulsen (2007) stated that the only detailed description of the plant was written by Heyne in 1927. It belongs to family

https://doi.org/10.35219/foodtechnology.2024.2.03

Zingiberaceae and comes from genus *Etlingera*. Its leaves are commonly used as cooking spices by local people.

Drying is applied to maintain product quality by inhibiting spoilage due to microorganisms and chemical reactions during storage (Roshanak *et al.*, 2016). Many studies have reported chemical changes in aromatic compounds after dehydration. Improper drying method accelerates cellular damages and causes loss of active compounds (Seeranguryar *et al.*, 2019). The use of different drying methods results in various drying rates, and for this reason, drying rate models are used to predict the precise time required to dehydrate leaves with a certain moisture level.

Compared to other chemical compositions, water has a prime impact on reaction and quality of foods (Al-Muhtaseb *et al*., 2002). In this case, water activity, which is expressed as a_w, can be used to control food stability since it may reduce microbial growth rate and chemical reactions (Basu *et al*., 2006). At a constant temperature, the relationship between moisture content and a_w is depicted in a moisture sorption isotherm (MSI), which reveals a non-linear line or a sigmoidal pattern in most food products, and these foods are classified as isotherm type II (Al-Muhtaseb *et al*., 2002). Moreover, MSI curve can be applied to estimate changes of food stability and shelf life and suggest suitable packaging (Basu *et al*., 2006). However, intensive studies discussing drying rate, MSI models, and the role of a_w on physical and chemical properties of *walang* leaves under different drying procedures have not been carried out. The aims of this work include determination of drying rate and MSI models and investigation of the roles of a_w on moisture content, color, TP, and AA of *walang* leaves dried by different methods (sun drying, sun drying with fan, air drying, fluidized bed drying). The research outcome is significant to industries for selecting the best drying method of *walang* leaves.

Materials and methods

Sample collection

Walang leaves were collected from a garden in Ciomas, Regency of Serang. The leaves with similar size were harvested, starting from those below the shoots to the fourth. They were placed in a bamboo-made container with banana leaves and then packed on a Styrofoam box containing ice gel bags. In the laboratory, they were washed, drained, and left for 45 min. A tissue paper was used to drain the remaining water on the leaves. The leaves were cut into 2×2 cm pieces and then packed in double-layered plastics and stored at the refrigerator prior to drying process in the following day.

Sampling procedure

The sampling points for all drying methods were determined by measuring weight reduction of leaves every 20 minutes during drying until a constant weight was achieved. The leaves during sun-drying (SD) and sun-drying with a fan (SDF) were directly dried under the sun. The drying conditions were recorded manually with an air quality monitor (TVOC HCHO PM2.5) and a digital anemometer (Hold Peak

HP-866B) every 15 minutes. The average temperature and air velocity were 35.61± 0.90 °C and 0.21 ± 0.02 ms^{-1} during SD process while the average temperature and air velocity were 33.92 ± 0.20 °C and 1.39 ± 0.00 ms^{-1} during SDF process. Fluidized bed drying (FBD) was operated at 34 ºC and at an air velocity of 2.8 ms^{-1} while air-drying (AD) was carried out at room temperature without airflow. The quantity of leaves used in each method was 90 g. A number of sampling points for each method were determined. For SD and FDB, 7 sampling points were taken (0, 1, 2, 3, 4, 5, 6 h). Meanwhile, 9 sampling points (0, 1, 2, 3, 4, 5, 6, 7, 8 h) at SDF process and 8 sampling points (0, 2, 4, 7, 13, 22, 31, 55 h) at AD process were taken.

Drying procedure

The leaves were freeze-dried (FD) in Benchtop Freeze Dryer at -47 ºC and vacuum pressure of 0.070 mBar for 72 h to reach constant weight. The leaves were directly dried under sun at average temperature of 35.61± 0.90 °C and average air velocity of 0.21 ± 0.02 ms^{-1} during sun-drying (SD) process. For sun-drying with fan (SDF), the leaves were dried at an average temperature of 33.92 ± 0.20 °C and an average air velocity of 1.39 ± 0.00 ms^{-1}. An air quality monitor (TVOC HCHO PM2.5) and a digital anemometer (Hold Peak HP-866B) were used to measure the drying conditions during SD and SDF processes. The temperature and air velocity were manually recorded every 15 minutes. Fluidized bed drying (FBD) was performed at 34 ºC and at an air velocity of 2.8 ms^{-1}. Meanwhile, air-drying (AD) was carried out at room temperature without airflow. The effect of each method was investigated at the quantity of leaves of 90 g.

Moisture content and water activity analysis

The fresh and dried *walang* leaves were analyzed for moisture content and water activity a_w. Moisture content was determined according to AOAC (2000), dried using an oven (Memmert, Germany) at 105±5 °C (AOAC, 2000). The a_w level was tested in a cup water activity analyzer (Aqualab 4TE, USA).

Mathematical models for drying

Five models for thin-layer drying were verified to depict drying curves of *walang* leaves (Table 1). Moisture ratio (MR) was calculated with equation 1.

$$\mathrm{MR} = \frac{\mathrm{Mt-Me}}{\mathrm{Mo-Me}} \tag{1}$$

where Mt, Mo, and Me referred to moisture content at time *t*, initial time, and equilibrium (kg moisture/kg dry matter), respectively, while *t* was time in minutes. Me values were relatively smaller than Mo values. Therefore, the MR equation was modified into MR=Mt/Mo (Izli *et al.*, 2014).

Mathematical model for MSI curve of *walang* leaves

Most models of MSI curves were proposed in literatures (Basu *et al.,* 2006). In this work, GAB, Oswin, Chen-Cleyton, Smith, Halsey, Henderson, and Caurie models were presented (Table 1) and applied to determine the most suitable models.

Table 1. Thin-layer drying (Mujaffar and John, 2018) and mathematical models for MSI curves (Dalgic *et al.*, 2012) of *walang* leaves.

Thin-layer drying model	Expression *	The MSI model	Expression
Lewis	MR = exp (-kt)	GAB	$X_{eq} = \dfrac{X_m C K a_w}{(1 - K a_w)(1 - K a_w + C K a_w)}$
Page	MR = exp ($-kt^n$)	Chen-Clayton	$a_w = \exp[-P1/(\exp P2Xeq)]$
Henderson and Pabis	MR = a exp (-kt)	Henderson	$\mathrm{Ln}[\ln(1/(1-a_w))] = \ln A + B \ln X_{eq}$
Peleg	MR = 1 – (x/(a + bx))	Caurie	$\dfrac{1}{X_{eq}} = \dfrac{1}{C_c X_m}\left(\dfrac{1 - a_w}{a_w}\right)$
Wang and Singh	MR = 1 + at + bt^2	Oswin	$X_{eq} = A\left(\dfrac{a_w}{1 - a_w}\right)$
		Smith	$X_{eq} = a + b \log(1-a_w)$
		Hasley	$a_w = \exp\left(\dfrac{-A}{{X_{eq}}^B}\right)$

* k is a drying rate constant, t is drying time (min), and a, b, n show empirical constants.

Color analysis

Color of fresh and dried leaves was expressed using CIE L*, a*, and b*. L* was used to describe the lightness of samples ranging from 100 (light) to 0 (dark). The a* showed a red (+) to green (-) intensity while b* indicated a yellow (+) and blue (-) intensity. Chroma showed color intensity and ΔE expressed total color changes. Color analysis (L*, a*, and b*) was performed by a chroma meter (Konica Minolta, USA). The total color changes (ΔE) and chroma were calculated using equations as follows (Seeranguryayar *et al.*, 2019):

$$\Delta E = \sqrt{(L^*_0 - L^*)^2 + (a^*_0 - a^*)^2 + (b^*_0 - b^*)^2} \qquad (2)$$

$$\text{Chroma (C)} = \sqrt{(a^{*2} + b^{*2})} \qquad (3)$$

Extraction of the bioactive compounds from leaves

Fresh and dried *walang* leaves were extracted, following a method prescribed by Mahirah *et al*. (2018). Briefly, sample powder (0.2 g) was added with 2 mL of methanol 80% in Erlenmeyer and stirred in an incubator shaker at 160 rpm for 24 h at room temperature. The mixture was filtered using a Whatman paper No. 1 to collect a clear extract. Total phenolic and antioxidant activity of the extracts were determined in accordance with the method described by Mahirah *et al*. (2018).

Statistical analysis

A duplicate measurement of samples was carried out and the results were presented as means ± standard deviation. The drying rate constant (*k*) was obtained from a curve plotting *ln* moisture content and drying time. The best-fitted thin-layer drying model and MSI model were evaluated based on determination coefficient (R^2), root mean square error (RMSE), and reduced chi-squared (χ^2). Mathematical models for R^2, χ^2, and RMSE (Izli *et al.*, 2014) were determined with equations 4, 5 and 6.

$$R^2 = 1 - \frac{\sum_1^n (XR_{i,exp} - XR_{i,pre})^2}{\sum_1^n (\overline{XR} - XR_{i,pre})^2} \quad (4)$$

$$\chi^2 = \frac{\sum_{i=1}^N (MR_{exp,i} - MR_{pre,i})^2}{(N-n)} \quad (5)$$

$$RMSE = \sqrt{\frac{\sum_{i=1}^N (MR_{pre,i} - MR_{exp,i})}{N}} \quad (6)$$

where $MR_{exp,i}$ is MR for experiment *i*; $MR_{pre,i}$ is a predicted MR for experiment *i*; N was number of data; n is number of constant in the equation.

The inflection point for moisture content, TP, and AA was determined from the second order of polynomials (García-Tejeda and Barrera-Figueroa, 2019). The inflection point for L*, a*, b*, ΔE, and chroma was collected from a_w exactly at the center of cavity on each curve. The best drying was determined from the sample at the end of each drying method and statistically analyzed by One-way ANOVA and Dunnet at a significance of 95% using IBM SPSS Statistics 26 (SPSS, Inc., Chicago, IL). Dried leaves (FD sample) were used as a control.

Results and discussion

Drying characteristics

Drying curves for *walang* leaves are presented in Figure 1. Moisture content (MC) decreased with the longer drying time *t* and this conformed to the drying curves for food and agriculture products. The sharp drop of moisture content at the initial step of drying coincided with the drastic rise in drying rate (DR). This means a loss of moisture content in the outer leaf surfaces. As seen in the curve, it is clear that the increase in drying temperature leads to a decline in MC. The result is in line with Ghanbarian *et al.* (2020) and Tarafdar *et al.* (2021). When a large difference in temperatures between matter and heat medium occurs, this accelerates heat transfer into the matter and as a consequence, water evaporates more quickly (Ummah *et al.*, 2016). Therefore, moisture loss in SD-treated samples is faster than in the other treatments. A high temperature in the daytime and a low relative humidity level improve the evaporation capacity in SD treatment (ELkhadraoui *et al.*, 2015). Based on One-way ANOVA, there are no significant effects of drying methods on MC at the end of drying ($p>0.05$). The MC, a_w, chroma, a*, b*, L*, ΔE, TP, and AA of the dried *walang* leaves at the end of each drying method are presented in Table 4.

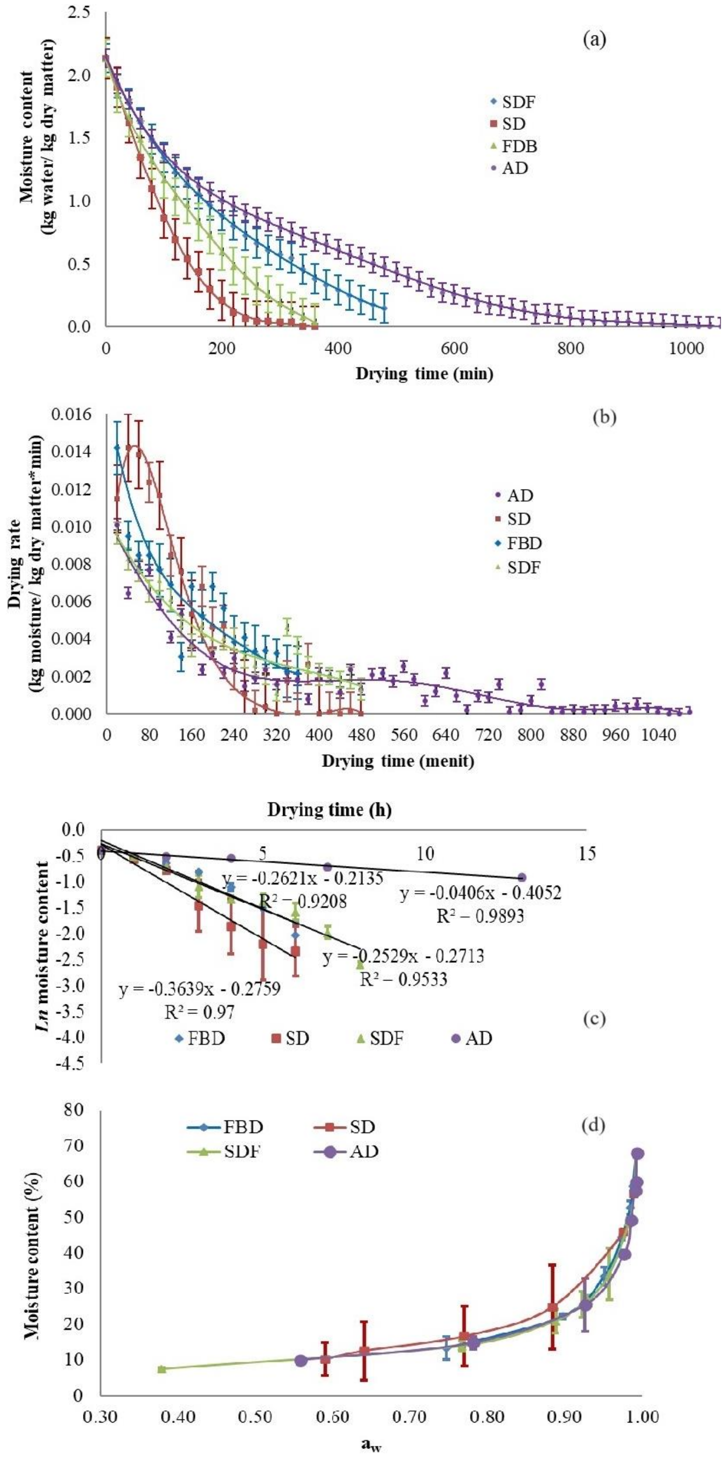

Figure 1. Changes in (a) moisture content, (b) drying rate over time, (c) constant of drying rate and (d) MSI curve for all drying methods.

The drying rate (DR) is expressed as the mass of moisture removed over time. In SD treatment, the drying rate reaches a maximum level and the sample becomes more dried following the declined drying rate. The falling rate period (FRP) for all drying methods is observed during the drying process, while a constant drying period (CRP) did not occur in the experiment. This shows that diffusion is the dominant physical mechanism governing moisture movement in the samples. In this work, the drying rate for SD treatment was higher than other treatments. Figure 1b clearly shows how DR is affected. The effect of drying temperature seems to be declined between 160 – 360 min of drying. The drying rate increased significantly at a higher temperature. This result is in accordance with the drying results of peppermint leaves (Ghanbarian *et al.*, 2020) and moringa leaves (Tarafdar *et al.*, 2021).

Relationship between *ln* moisture content and drying time is used to determine constant *k*. As depicted in Figure 1c, the constant *k* expresses the rate of water diffused from the matter and it may represent the drying period (Ummah *et al*., 2016). In this case, the SD method shows the quickest process since it applies the highest temperature (35.61± 0.90 °C). The higher temperature would increase the *k* value as more heat is transferred which leads to an intensified evaporation rate (Ummah *et al*., 2016).

Mathematical models of drying rate

The drying effectivity can be improved by developing drying time estimation through the drying rate model. In this study, some mathematical models are used, i.e. Lewis, Page, Henderson and Pabis, Peleg, and Wang and Singh. These models are simple to use and often applied in the thin-layer drying process for leaves. Page model is known to be the best for drying 13 types of leaves (Babu *et al.,* 2018). Constants of the equation, R^2, RMSE, and X^2 are summarized in Table 2. Wang and Singh model is the most suitable to the experimental data for all drying methods.

Mathematical models of MSI

The MSI curve depicts the relationship between MC and equilibrium relative humidity (RH) in a storage room or a_w value at a certain temperature (Al-Muhtaseb *et al.,* 2002). The term “sorption” refers to a process in which a solid food matter and water molecules combine reversibly through physical and chemical adsorption processes and capillary condensation. Other factors affecting the MSI curve include food components including carbohydrates, protein, fats, and minerals (Basu *et al*., 2006).

As depicted in Figure 1d, the curve is classified as type II with a sigmoidal shape. The sigmoidal shape results from the huge amount of water binding in the leaves (Basu *et al.,* 2006). The moisture content of all curves dropped heavily at zone III and this stopped at the inflection point (Table 3). Type III water is defined as free water and bound water (Basu *et al.*, 2006) and such properties make it easily evaporate at zone III. In this work, water release after the inflection point occurred slowly.

Table 2. Parameters for equations of drying rate, MSI, R^2, RMSE, and X^2 of *walang* leaves.

Model		FBD	SD	SDF	AD
Parameters of drying rate					
Lewis	k	0.2604	0.3472	0.2526	0.0369
	R^2	0.9228	0.976	0.9525	0.9585
	RMSE	0.1506	0.1088	0.1457	0.1349
	X^2	0.0318	0.0166	0.0273	0.0243
Page	k	2.1186	1.707	1.932	2.8362
	n	1.3436	1.3881	1.2585	0.8947
	R^2	0.9599	0.9755	0.9815	0.9837
	RMSE	0.1661	0.1331	0.1137	0.1255
	X^2	0.0414	0.0266	0.0172	0.0221
Henderson and Pabis	a	1.1834	1.1064	1.1218	0.9238
	k	0.26	0.347	0.253	0.037
	R^2	0.9192	0.9585	0.976	0.9865
	RMSE	0.0935	0.0660	0.0537	0.0454
	X^2	0.0055	0.0038	0.0014	0.0017
Peleg	a	3.6	32	-15	6.67
	b	1.356	-3.61	3.82	5
	R^2	0.9932	0.9379	0.9544	0.8644
	RMSE	0.0290	0.0926	0.0923	0.4977
	X^2	0.0012	0.0120	0.0110	0.3303
Wang and Singh	a	-0.0051	0.0183	0.0084	0.0004
	b	-0.104	-0.2623	-0.1754	-0.0362
	R^2	0.9975	0.9782	0.9837	0.9974
	RMSE	0.0151	0.0626	0.0375	0.0393
	X^2	0.0004	0.0068	0.0021	0.0025
Parameters of MSI curve					
GAB	Xm	0.028	0.052	0.035	0.035
	C1	-1.153	56.108	-2.593	-2.593
	K	0.991	0.970	0.980	0.980
	R^2	0.999	0.9861	0.9806	0.9859
	RMSE	0.0455	0.2024	0.2104	0.0637
	X^2	0.0036	0.0717	0.0664	0.0637
Hasley	A	51.93	50.00	58.27	64.522
	B	1.4216	1.5853	1.5183	1.5753
	R^2	0.9988	0.9937	0.9927	0.9864
	RMSE	0.0187	0.0575	0.0557	0.0804
	X^2	0.0005	0.0046	0.0040	0.0086
Henderson	A	3.8325	3.6774	4.124	3.9805
	B	0.4775	0.619	0.6448	0.5941
	R^2	0.9625	0.9742	0.8631	0.9273
	RMSE	0.0809	0.1058	0.2535	0.1664
	X^2	0.0092	0.0157	0.0826	0.0369
Oswin	A	14.41	10.063	11.619	11.729
	B	0.6779	0.5931	0.5989	0.5916
	R^2	0.9975	0.9946	0.9815	0.9825
	RMSE	0.0428	0.0772	0.1341	0.1324
	X^2	0.0026	0.0083	0.0231	0.0233

While the inflection point of SD, SDF, and AD was found at zone II, the inflection point of FBD occurred at zone III. Although zone II began at a_w of <0.84, the water at a_w below the inflection point of FBD possibly represented the transition from free water to bound water. Even though water molecule binding at zone II was weaker than that at zone I, it had a slightly higher level of evaporation enthalpy than pure water (Basu *et al.*, 2006). This may explain why the water evaporates more slowly after the inflection point.

The inflection point for SD treatment as shown in Table 3 was the lowest (0.7412). The higher average temperature of SD (35.61± 0.90 °C) evaporated more water. As the drying time for SDF and AD was longer than FBD, more water was evaporated. Consequently, their inflection point was lower. At the end of drying, water activity ranged from 0.7472 to 0.3787, which was found in zone II. The a_w of <0.6 might indicate higher stability of *walang* leaves (Fennema, 1996). Based on the One-way ANOVA test, drying methods significantly influenced the water activity of the leaves at the end of the drying process ($p<0.05$), and the value was not different significantly from the water activity of FD-treated samples ($p>0.05$) according to Dunnet test (Table 4).

The MSI curve was then compared to the other models including Hasley, Chen Clayton, Henderson, Caurie, Oswin, Smith, and GAB because each model has a wide range of water activity values (Al-Muhtaseb *et al.*, 2002). Chen Clayton, Caurie, and Smith models had R^2 <0.9. In general, models with R^2 > 0.97 were considered suitable for explaining the drying data (Babu *et al.*, 2018). Table 2 summarizes isotherm models, equation constant, R^2, RMSE, and X^2. As a result, the GAB model conformed to the MSI curve of leaves dried by FBD while the Hasley model was good for SDF and AD treatments and Oswin was suitable for SD.

Color changes

The relationship between a_w and chroma, a*, b*, L*, and ΔE is presented in Figure 2. The rise of a_w value is in line with the increase in b* and chroma values observed in all drying methods and their increment occurs suddenly after the inflection point (Table 3). Meanwhile, L*, a*, and ΔE values obtained from four drying methods decreased with the rise of a_w value. Attributes L*, a*, and ΔE immediately dropped after the inflection point (Table 3). Meanwhile, a sharp increase in b* and chroma as well as a sharp decline of L*, a*, and ΔE occurred at zone III. In the third zone, water was reported able to act as solvent and it could speed up the rate of various reactions (Fennema, 1996). This may explain the dramatic rise of b* and chroma and the sharp decline of L*, a*, and ΔE in a_w at zone III.

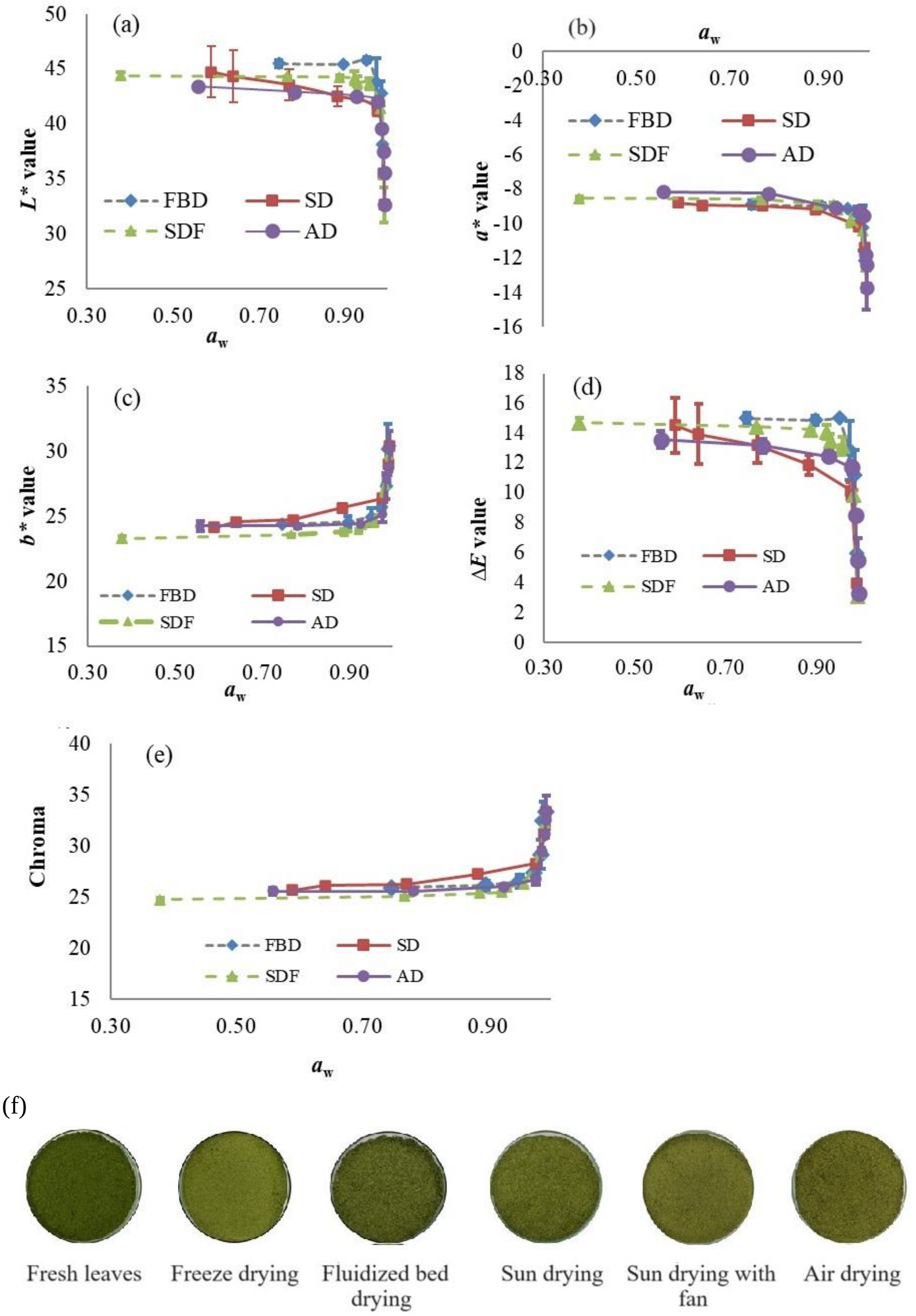

Figure 2. Color changes as affected by water activity in dried samples (a–e) and physical appearances of samples dried (f) for all drying methods.

The loss of b* value results in darker appearances on the dried leaves (Figure 2f). The green color of leaves is caused by abundant chlorophyll pigment. During the drying process, the pigment degrades into other substances, and non-enzymatic processes may also occur, resulting in dark color (Seerangurayar *et al*., 2019). In this work, the samples treated by FBD were greener and this may relate to the absence of exposure to sunlight. The sunlight is a main factor contributing to dark colors. The average day temperature reached 36.92 °C in SD and it was higher than the temperature in FBD. The high temperature is able to more quickly degrade colors in the SD method due to a high level of energy transfer to the foods (Guiné and Barroca, 2012). The increased L* results from the decline of moisture content and this produces an opaque appearance, resulting in stronger light reflection. Color changes are a complex phenomenon and their kinetics depend highly on moisture content (Seerangurayar *et al*., 2019). The result is in accordance with previous works, including green tea dried by sun drying by Roshanak *et al.* (2016) and lemongrass leaves dried by tray drying by Mujaffar and John (2018).

Table 3. Water activity value (a_w) of walang leaves at the inflection point.

Drying methods	Water activity (a_w)						
	MC	**TP**	**L***	**a***	**b***	**ΔE**	**Chroma**
FBD	0.8896	0.9318	0.9738	0.9738	0.9738	0.9738	0.9738
SD	0.7412	0.7646	0.9760	0.9760	0.9760	0.9760	0.9760
SDF	0.7434	0.9375	0.9579	0.9579	0.9579	0.9579	0.9579
AD	0.8081	0.8277	0.9768	0.9768	0.9768	0.9768	0.9768

The results of chroma showed that leaves dried in FBD (−22.17%) had the highest color stability followed by SD (−22.93%), AD (−23.28%), and SDF (-25.75%) dried leaves. The darker appearance of SDF dried leaves might be due to direct sunlight exposure and the longer drying time (8 h) compared to SD (6 h) and FBD (6 h) dried leaves. The higher air flow rate in SDF (1.39 ± 0.00 m/s) compared to SD (0.21 ± 0.02 m/s) and AD (0 m/s) also caused faster color degradation of leaves dried by SDF. Meanwhile, fluidized bed drying (FBD) and air-drying (AD) were carried out in a room without sunlight exposure. The direct sunlight exposure and the higher air flow rate were able to cause faster color degradation which reduces the chroma value (Seeranguravar *et al*., 2019). Regarding total color changes, ΔE values are high and they indicate that all drying methods are unable to retain the colors of fresh leaves. Total color change (ΔE) was used to measure the overall color difference between fresh and dried leaves. However, all drying procedures significantly affected the color attributes (L*, a*, b*, and ΔE) of the dried leaves ($p<0.05$). Meanwhile, in all drying methods, the Dunnet test (Table 4) showed that L* and ΔE of the dried leaves differed from those dried by FD ($p<0.05$). In terms of a*, b*, and chroma, the results were not different from those in FD samples ($p>0.05$).

Effects of water activity on total phenolic content

The total phenolic content (TP) of the four dried samples greatly increased (350.49 – 808.60 mg GAE/100 g dm) with the lower level of water activity (0.9931 – 0.3787) as shown in Figure 3a. The TP values in all five dried samples were higher than those in fresh samples. Figure 3a showed that TP dramatically rose in a_w levels at zone III and after the inflection point (Table 3). Water properties at zone III could explain how TP could extremely increase in that zone. Moreover, the surge of TP could be caused by other factors, including (1) cleavages of phytochemical bonds from cellular structures during drying (Yap *et al.*, 2022), (2) formation of compounds that better respond to Folin-Ciocalteu (Garcia *et al*., 2021), and (3) low water activity in dry samples that inhibits enzymatic oxidation reaction and abundant amount of phenolic in extracts (Mondaca *et al.,* 2018).

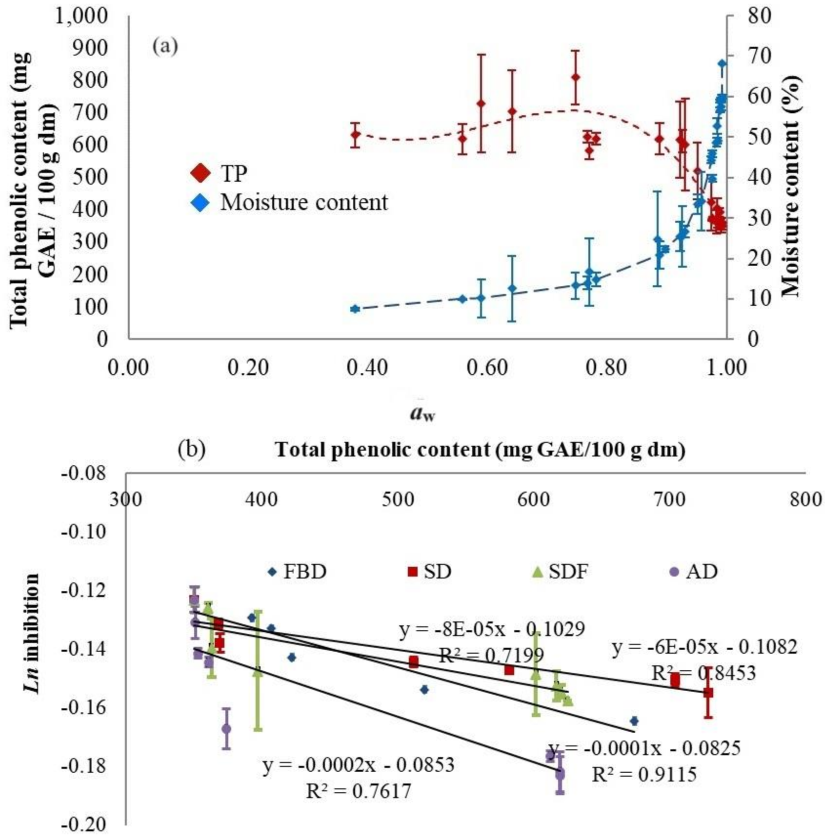

Figure 3. Relationship between MSI (a) and *Ln* of inhibition value (b) with TP for different drying methods.

After reaching the inflection point, the rise of TP content in all four drying treatments did not progress linearly, stemming from the scarcity of moisture content which facilitates hydrolysis reaction. The TP content increased as more low molecular weight compounds were formed; this happens because complex phenolic compounds, such as tannin and lignin, hydrolyze greatly (Al-Farsi *et al.,* 2005). The higher average temperature for SD evaporates a larger amount of water and therefore its inflection point is lower than the other methods. The lower drying temperature for AD evaporates water more slowly than FBD and SDF. As a consequence, there is a sufficient amount of water for hydrolyzing complex phenolic compounds and this is the main reason why the inflection point for AD (0.8277) was lower than that for FBD (0.9318) and SDF (0.9375) as shown in Table 3.

In this experiment, the total phenolic content of leaves dried by FD was the highest (1212.88 ± 55.62 mg GAE/100 g dm) as shown in Table 4. During FD, all leaves were dried at -47 ºC, thereby preventing them from degradation reaction and encouraging the formation of small ice crystals in the cells as well as rapid removal of ice crystals from the cells. The rapid release of ice crystal maintains cellular structures, thereby preserving the content of phenolic and vitamins (Klungboonkrong *et al*., 2018).

The dried leaves obtained through FBD and SD processes had a higher level of TP than those treated by SDF and AD whose TP content increased more slowly after the inflection point. Drying time and temperature markedly affect the retention of phenolic compounds. Longer drying processes and lower temperatures in SDF and AD increased the exposure of materials to enzymatic reactions and oxidation (Heras *et al*., 2014). The rise of TP in leaves under higher drying temperature possibly related to the formation of phenolic compounds through the Maillard reaction (Mouhoubi *et al*., 2021). The One-way ANOVA test showed that drying methods significantly influenced TP content ($p<0.05$) while the Dunnet test also revealed significant differences between four drying treatments and FD ($p<0.05$) (Table 4).

Effects of water activity on antioxidant activity

Figure 3b shows high correlation ($R^2>0.7$) between TP and AA where the antioxidant activity of samples in the four methods decreased with the rise of TP. This explains that the compounds may lose their ability to scavenge free radicals. Although TP content of the dried leaves increased, their AA seemed to decrease. Basically, the antioxidative properties of foods relied on the mixture of their chemical substances with various polarity, including vitamins, carotenoids, and polyphenols. When the sample was extracted, their AA was dependent on types and quantity of antioxidative compounds. Drying typically reduces antioxidant activity due to heat exposure (Rafiq *et al.,* 2019).

The decrease in AA may partially result from the reduction reaction, oxidative degradation, and polymerization-condensation reaction of compounds, which reduce the capacity of antioxidant compounds to donate hydrogen (Yap *et al.*, 2022). Degradation or transformation of polyphenol compounds was able to form non-antioxidant compounds during drying (Rafiq *et al.*, 2019). The reaction was also reported able to change the composition of phenolic compounds (Liu *et al.,* 2019). Therefore, despite having a low content of TP in fresh leaves, their antioxidant activity could be still higher (88.42%) as shown in Figure 3b.

The dried leaves of SD treatment had a higher level of AA than the other methods. The reason behind this finding may relate to faster water evaporation, thus retarding the degradation of antioxidant compounds. Drying temperature is also reported able to affect AA where at a higher temperature the melanoid was intensively produced and accumulated, leading to the rise of AA (Mouhoubi *et al*., 2021). In addition, disruption of cell walls may release antioxidant compounds and this is favorable for antioxidant compounds (Zannou *et al*., 2021). The decline of AA with higher content of TP and lower level of AA than fresh leaves was reported in some drying studies, including FD (Klungboonkrong *et al*., 2018; Kopec and Piatkowska, 2022), SD (Al-Farsi *et al.*, 2005), and AD (Al-Farsi *et al.*, 2005). Meanwhile the drop of AA in other drying processes was reported by Liu *et al.* (2019) and Yap *et al.* (2022).

In this case, FD samples had a lower level of AA than SD samples and fresh leaves (Table 4). Freeze drying was found to significantly reduce the content of bioactive compounds in *Citrus maxima* (Vanamala *et al.*, 2005) and red pummelo (Tsai *et al.*, 2007). Meanwhile, AD treatment resulted in the lowest AA, caused by drying time and temperature that made the samples more intensively exposed to enzymatic and oxidation reactions. One-way ANOVA test revealed that drying methods did not affect AA of the samples at the end of drying ($p>0.05$), while the Dunnet test showed that there were no significant differences in AA between samples treated by SD, SDF, and AD and those treated by FD ($p>0.05$).

Table 4. The MC, a_w, chroma, a*, b*, L*, ΔE, TP, AA of the dried *walang* leaves at the end of each drying methods.

Methods	FD	FBD	SD	SDF	AD
MC (%)	5.39 ±0.00	13.30 ±0.03	10.20 ±0.05	7.50±0.00	10.02±0.00
a_w	0.1322±0.02	0.7472±0.01	0.5897±0.25	0.3787±0.03	0.5579±0
L*	50± 1.13[b]	45.49±0.33[a]	44.74±2.31[a]	44.38±0.31[a]	43.38±0.48[a]
a*	-13.69 ±2.21	-8.90 ±0.23	-8.78 ±0.18	-8.53 ±0.09	-8.14 ±0.05
b*	19.62± 1,20	24.35±0	24.13±0.28	23.22±0.20	24.23±0.38
ΔE	20.56±0.37[b]	14.99±0.36[a]	14.52±1.87[a]	14.69±0.32[a]	13.58±0.58[a]
Chroma	23.95± 2.25	25.93± 0.08	25.68± 0.20	24.74± 0.15	25.56± 0.38
TP (mg GAE/100 g dm)	1212.8±55.6[b]	808.6±81.8[a]	728.2±151.3[a]	630.6±38.9[a]	619.3±46.6[a]
AA (%)	85.22 ±0	80.30±0.03	85.66 ±0.01	81.20 ±0.02	83.28 ±0.01

Different letters on a row indicate that values are significantly different ($p<0.05$).

Conclusions

Wang and Singh's model gave the best result for describing the drying properties of *walang* leaves. MSI curve for SDF and AD best fitted to Hasley model, and SD and FBD followed Oswin and GAB models. Water activity affected moisture content, TP, AA, and color. Moisture content for all samples dropped sharply at zone III (0.7412 – 0.8896). While there was a surge in ΔE, a*, and L* (0.9579 – 0.9738), the b* and chroma values (0.9579 – 0.9738) decreased markedly at zone III. Total phenolic content was higher in dried samples than in fresh leaves, but a converse effect was found for antioxidant activity. A sharp increase in TP (0.7646 – 0.9375) was also found at zone III. The TP, L* and ΔE of the dried leaves were different significantly from those dried by FD ($p<0.05$) according to the Dunnet test while moisture content, water activity, a*, b*, and chroma were not different from those in FD samples ($p>0.05$). Dunnet test also revealed that there were no significant differences in AA between samples treated by SD, SDF, and AD and those treated by FD ($p>0.05$). This study clearly showed that water activity is a determinant of the physical and chemical properties of the *walang* leaves during drying. The antioxidant activity of samples in the SD method was comparable with those treated with FD, but the SD process showed the quickest drying rate. Therefore, drying by SD is a potential drying method and is recommended for *walang* leaves.

Acknowledgments

The authors would like to thank the Indonesia Endowment Fund for Education, Ministry of Finance of the Republic of Indonesia for the scholarship to SM and the research funding. The authors also would like to thank to Department of Food Science and Technology, Bogor Agricultural University, which has provided equipment and instruments for this research.

References

Al-Farsi, M., Alasalvar, C., Morris, A., Baron, M., Shahidi, F. 2005. Comparison of antioxidant activity, anthocyanins, carotenoids, and phenolics of three native fresh and sun-dried date (*Phoenix dactylifera* L.) varieties grown in Oman. *Journal of Agricultural and Food Chemistry*, **53**(19), 7592–7599.

Al-Muhtaseb, A.H., McMinn, W.A.M., Magee, T.R.A. 2002. Moisture sorption isotherm characteristics of food products: a review. *Food and Bioproducts Processing*, **80**(2), 118–128.

Babu, A.K., Kumaresan, G., Raj, V.A.A., Velraj, R. 2018. Review of leaf drying: Mechanism and influencing parameters, drying methods, nutrient preservation, and mathematical models. *Renewable and Sustainable Energy Reviews*, **90**(2018), 536–556.

Basu, S., Shivhare, U.S., Mujumdar, A.S. 2006. Models for sorption isotherms for foods: a review. *Drying Technology: An International Journal*, **24**(8), 917–930.

Dalgıc, A.C., Pekmez, H., Belibagli, K.B. 2012. Effect of drying methods on the moisture sorption isotherms and thermodynamic properties of mint leaves. *Journal of Food Science and Technology*, **49**(4), 439–449.

ELkhadraoui, A., Kooli, S., Hamdi, I., Farhat, A. 2015. Experimental investigation and economic evaluation of a newmixed-mode solar greenhouse dryer for drying of red pepper and grape. *Renewable Energy*, **77**(2015), 1–8.

Fennema, O.R. 1996. *Food Chemistry*, 42–54. Marcel Dekker, Inc., New York.

Garcia, L.M., Ceccanti, C., Negro, C., De Bellis, L., Incrocci, L., Pardossi, A., Guidi, L. 2021. Effect of drying methods on phenolic compounds and antioxidant activity of *Urtica dioica* L. leaves. *Horticulturae*, **7**(10), 1–12.

García-Tejeda, Y.V., Barrera-Figueroa, V. 2019. Least squares fitting-polynomials for determining inflection points in adsorption isotherms of spray-dried açaí juice (*Euterpe oleracea* Mart.) and soy sauce powders. *Powder Technology*, **342**(2019), 829–839.

Ghanbarian, D., Torki-Harchegani, M., Sadeghi, M., Pirbalouti, AG. 2020. Ultrasonically improved convective drying of peppermint leaves: Influence on the process time and energetic indices. *Renewable Energy*, **153**(2020), 67–73.

Guiné, R.P., Barroca, M.J. 2012. Effect of drying treatments ontexture and color of vegetables (pumpkin and green pepper). *Food and Bioproducts Processing*, **90**(1), 58–63.

Heras, R.M., Heredia, A., Castello, M.L., Andres, A. 2014. Influence of drying method and extraction variables on the antioxidant properties of persimmon leaves. *Food Bioscience*, **6**(2014), 1–8.

Izli, N., Yıldız, G., Unal, H., Isık, E., Uylaser, V. 2014. Effect of different drying methods on drying characteristics, colour, total phenolic content, and antioxidant capacity of goldenberry (*Physalis peruviana* L.). *International Journal of Food Science and Technology*, **49**(1), 9–17.

Klungboonkrong, V., Phoungchandang, S., Lamsal, B. 2018. Drying of *Orthosiphon aristatus* leaves: Mathematical modeling, drying characteristics, and quality aspects. *Chemical Engineering Communications*, **205**(9), 1239–1251.

Kopec, B.R., Piatkowska, E. 2022. Total polyphenols and antioxidant properties of selected fresh and dried herbs and spices. *Applied Sciences*, **12**(10), 4876.

Liu, X., Yan, X., Bi, J., Wu, X., Liu, J., Zhou, M. 2019. Identification of phenolic compounds and antioxidant activity of guava dehydrated by different drying methods. *Drying Technology*, **38**(8), 987–1000.

Mahirah, S.Y., Rabeta, M.S., Antora, R.A. 2018. Effects of different drying methods on the proximate composition and antioxidant activities of *Ocimum basilicum* leaves. *Food Research*, **2**(5), 421–428.

Mondaca, R.L., Gálvez, A.V., Rojas, P., Stucken, K., Delporte, C., Barra, G.V., Jagus, R.J., Agüero, M.V., Pasten, A. 2018. Antioxidant, antimicrobial and anti-inflammatory potential of *Stevia rebaudiana* leaves: effect of different drying methods. *Journal of Applied Research on Medicinal and Aromatic Plants*, **11**(2018), 37–46.

Mouhoubi, K., Makhlouf, L.B., Mehaba, W., Himed-Idir, H., Madani, K. 2021. Convective and microwave drying of coriander leaves: Kinetics characteristics and modeling, phenolic contents, antioxidant activity, and principal component analysis. *Journal of Food Process Engineering*, **45**(1), 1–13.

Mujaffar, S., John, S. 2018. Thin-layer drying behavior of West Indian lemon grass (*Cymbopogan citratus*) leaves. *Food Science and Nutrition*, **6**(4), 1085–1099.

Poulsen, A.D. 2007. *Etlingera giseke* of Java. *Gardens Bulletin of Singapore*, **59**,145–172.

Rafiq, S., Singh, B., Gat, Y. 2019. Effect of different drying techniques on chemical composition, color and antioxidant properties of kinnow (*Citrus reticulata*) peel. *Journal of Food Science and Technology*, **56**(5), 2458–2466.

Roshanak, S., Rahimmalek, M., Goli, S.A.H. 2016. Evaluation of seven different drying treatments in respect to total flavonoid, phenolic, vitamin C content, chlorophyll, antioxidant activity and color of green tea (*Camellia sinensis* or C. assamica) leaves. *Journal of Food Science and Technology*, **53**(1), 721–729.

Seerangurayar, T., Al-Ismail, A.M., Jeewantha, L.H.J., Al-Habsib, N.A. 2019. Effect of solar drying methods on color kinetics and texture of dates. *Food and Bioproducts Processing*, **116**(2019), 227–239.

Tarafdar, A., Jothi, N., Kaur, B.P. 2021. Mathematical and artificial neural network modeling for vacuum drying kinetics of *Moringa olifera* leaves followed by determination of energy consumption and mass transfer parameters. *Journal of Applied Research on Medicinal and Aromatic Plants*, **24**(100306), 1–8.

Tsai, H., Chang, S.K.C., Chang, S. 2007. Antioxidant content and free radical scavenging ability of fresh red pummelo (*Citrus grandis* (L.) Osbeck] juice and freeze-dried products. *Journal of Agricultural and Food Chemistry*, **55**(8), 2867–2872.

Ummah, N., Yohanes, A.P., Ani, S. 2016. Determination of the drying rate constant of shallot (*Allium ascalonicum* L.) slice using tunnel dehydrator. *Journal of Agro-based Industry*, **33**(2), 49–56.

Vanamala, J., Cobb, G., Turner, N.D., Lupton, J.R., Yoo, K.S., Pike, L.M., Patil, B.S. 2005. Bioactive compounds of grapefruit (*Citrus paradisi* Cv. Rio Red) respond differently to postharvest irradiation, storage, and freeze drying. *Journal of Agricultural and Food Chemistry*, **53**(10), 3980–3985.

Yap, E.S.P, Uthairatanakij, A., Laohakunjit, N., Jitareerat, P. 2022. Influence of hot air drying on capsaicinoids, phenolics, flavonoids and antioxidant activities of `Super Hot' chilies. *PeerJ*, **10**(e13423), 1–25.

Zannou, O., Pashazadeh, H., Ghellam, M., Hassan, A.M.A., Koca, I. 2021. Optimization of drying temperature for the assessment of functional and physical characteristics of autumn olive berries. *Journal of Food Processing and Preservation*, **45**(9), e15658.